

Unsupervised Contrastive Learning Using Out-Of-Distribution Data for Long-Tailed Dataset

Cuong Manh Hoang^a, Yeejin Lee^b, Byeongkeun Kang^{c,*}

^aDepartment of Electronic Engineering, Seoul National University of Science and Technology, 232 Gongneung-ro, Nowon-gu, Seoul, 01811, South Korea

^bDepartment of Electrical and Information Engineering, Seoul National University of Science and Technology, 232 Gongneung-ro, Nowon-gu, Seoul, 01811, South Korea

^cSchool of Electrical and Electronics Engineering, Chung-Ang University, 84 Heukseok-ro, Dongjak-gu, Seoul, 06974, South Korea

Abstract

This work addresses the task of self-supervised learning (SSL) on a long-tailed dataset that aims to learn balanced and well-separated representations for downstream tasks such as image classification. This task is crucial because the real world contains numerous object categories, and their distributions are inherently imbalanced. Towards robust SSL on a class-imbalanced dataset, we investigate leveraging a network trained using unlabeled out-of-distribution (OOD) data that are prevalently available online. We first train a network using both in-domain (ID) and sampled OOD data by back-propagating the proposed pseudo semantic discrimination loss alongside a domain discrimination loss. The OOD data sampling and loss functions are designed to learn a balanced and well-separated embedding space. Subsequently, we further optimize the network on ID data by unsupervised contrastive learning while using the previously trained network as a guiding network. The guiding network is utilized to select positive/negative samples and to control the strengths of attractive/repulsive forces in contrastive learning. We also distil and transfer its embedding space to the training network to maintain balancedness and separability. Through experiments on four publicly available long-tailed datasets, we demonstrate that the proposed method outperforms previous state-of-the-art methods.

Keywords: Unsupervised contrastive learning, Self-supervised learning, Long-tailed data, Imbalanced data, Convolutional neural networks.

1. Introduction

Self-supervised learning (SSL) is an important research topic because it enables learning representations without human-annotated labels. These learned representations are subsequently utilized in downstream tasks to reduce annotation efforts and improve accuracy (Biswas et al., 2024; Chai et al., 2024; Yin et al., 2025; Wen et al., 2025; Logacjov and Bach, 2024; Akrim et al., 2023). For instance, once a backbone network is trained using SSL, a head network with fewer parameters can be appended to the frozen backbone and learned using a smaller dataset to address a downstream task. More specifically, to achieve robust accuracy given a small dataset, we can employ SSL to initially train a backbone network on unlabeled images from the web. Then, we append a head network to the backbone and train the head on the small target dataset. Accordingly, SSL is effective in various applications where data for target tasks are insufficient to learn effective representations. These applications include not only areas where data is hard to collect such as natural disasters or medical domains but also general tasks involving less-frequent objects such as tigers, irons, and operating scissors. Due to its significance, numerous researchers

have investigated various methods to embed meaningful and balanced representations by training networks without human annotations (Liu et al., 2023; Tian et al., 2021).

While previous SSL methods have demonstrated their effectiveness in learning representations without labels on balanced and curated datasets, they have achieved limited performance on imbalanced datasets (Liu et al., 2022). In Table 1, we also experimentally demonstrate the challenge caused by long-tailed data. We train models using a popular self-supervised learning method, SimCLR (Chen et al., 2020), on a balanced subset and a long-tailed subset of the CIFAR-10 and CIFAR-100 datasets (Cui et al., 2019). Although both subsets contain the same total number of images, the distributions of the number of images for classes are different (balanced vs. imbalanced). For the long-tailed subset, we use an imbalance ratio of 100. As shown in the table, the models trained on the balanced subsets achieve higher overall accuracies and better balancedness (lower standard deviation) for both datasets. This limitation is critical because the real world contains numerous objects, and their distributions are inherently imbalanced (Xiang et al., 2024; Shi et al., 2024b; Wang and Zhai, 2024; Pang et al., 2023; Fan et al., 2022; Zhang et al., 2024; Lu et al., 2024). Therefore, this paper addresses the problem of learning balanced and meaningful representations on long-tailed datasets.

Due to the importance of SSL on long-tailed datasets, researchers have explored various approaches. These approaches

*Corresponding author.

Email addresses: cuonghoang@seoultech.ac.kr (Cuong Manh Hoang), yeejinlee@seoultech.ac.kr (Yeejin Lee), byeongkeunkang@cau.ac.kr (Byeongkeun Kang)

Table 1: Comparison of models trained on a balanced subset D_b and a long-tailed subset D_l from the CIFAR-10 and CIFAR-100 datasets (Cui et al., 2019). Additional details on the evaluation metrics and protocols are provided in Section 4.1.

Dataset	Subset	Many \uparrow	Med. \uparrow	Few \uparrow	STD \downarrow	All \uparrow
CIFAR-10	D_b	85.43	85.96	82.33	1.87	84.62
	D_l	82.40	73.91	70.19	5.11	75.34
CIFAR-100	D_b	48.97	48.69	47.56	0.63	48.41
	D_l	51.50	45.58	45.96	2.71	47.65

include applying strong regularization to rare samples (Liu et al., 2022), leveraging network pruning to discover tail samples (Jiang et al., 2021b), utilizing the memorization effect to find rare samples (Zhou et al., 2022), and using unlabeled out-of-distribution (OOD) datasets to rebalance tail samples (Bai et al., 2023).

In long-tailed learning, one conventional approach rebalances the data distribution by re-sampling data from tail classes (Japkowicz and Stephen, 2002). However, over-sampling tail samples often leads to overfitting due to the limited diversity of samples in those classes. To address this issue, another method employs under-sampling for head classes while over-sampling for tail classes with synthetic data (Chawla et al., 2002). While synthetic data mitigate overfitting, they are error-prone due to noise introduced during data synthesis (Drummond and Holte, 2003; Cui et al., 2019). Consequently, researchers have investigated leveraging unlabeled in-distribution data to rebalance the data distribution (Yang and Xu, 2020). Although this approach improves long-tailed learning, collecting sufficient in-distribution data is challenging. As a result, recent studies have explored using unlabeled out-of-distribution data and demonstrated its effectiveness in addressing these challenges (Wei et al., 2022; Bai et al., 2023).

Therefore, in this paper, we also investigate SSL on an unlabeled long-tailed dataset by leveraging unlabeled OOD data, considering prevalent online data without labels. However, different from (Bai et al., 2023), we propose a two-step framework based on the hypothesis that using OOD data throughout the entire training might degrade accuracy because generating accurate pseudo-labels for the combined data is more challenging than that for only ID data. In the proposed framework, we firstly pre-train a network using both in-domain (ID) data and sampled OOD data to learn a balanced and well-separated embedding space. This step comprises tail sample discovery, OOD data sampling, and training to learn the embedding space. Subsequently, we utilize the pre-trained network to further optimize the network for the ID dataset. It involves employing the pre-trained network to select positive/negative samples and to control the strengths of attractive/repulsive forces in contrastive learning. Additionally, we distil the balanced and well-separated embedding space from the pre-trained network and transfer it to the training network.

The contributions of this paper are summarized as follows: (1) We present, to the best of our knowledge, the first SSL method for a long-tailed dataset that leverages a pre-trained network on OOD and ID data; (2) To learn a balanced and

well-separated embedding space, we first train a network using the proposed pseudo semantic discrimination loss alongside a domain discrimination loss on both ID and carefully sampled OOD data; (3) We then leverage the pre-trained network to further optimize the network for an ID dataset. We propose to employ the pre-trained network to select positive/negative samples and to control the strengths of attractive/repulsive forces in contrastive learning. Additionally, we distil the balanced space from the pre-trained network and transfer it to the training network; (4) We demonstrate the effectiveness of the proposed method by freezing the further optimized network, appending a linear classifier to the frozen network, and training/evaluating on a long-tailed dataset.

2. Related Work

2.1. Self-Supervised Learning with Long-Tailed Datasets

Yang and Xu (2020) explored using self-supervised pre-training to mitigate label biases in class-imbalanced datasets. They demonstrated that classifiers pre-trained with self-supervised learning (SSL) consistently outperform their supervised learning counterparts for such datasets. Their SSL methods utilized rotation prediction (Gidaris et al., 2018) and Momentum Contrast (MoCo) (He et al., 2020).

To address biases caused by class imbalance, Liu et al. (2022) introduced a re-weighted regularization method. This method begins by estimating the density of examples using a kernel estimation approach and subsequently applies strong regularization to the estimated rare samples using the Sharpness-Aware Minimization (SAM) technique (Foret et al., 2021). As an alternative method for estimating long-tail examples, Jiang et al. (2021b) proposed using network pruning instead of kernel density estimation. This approach is based on the observation that network pruning has more impact on difficult-to-learn samples than easier ones. In detail, they introduced Self-Damaging Contrastive Learning (SDCLR), which emphasizes tail samples in a contrastive loss by utilizing a trained model and its pruned version. To enhance the discovery of tail samples, Zhou et al. (2022) leveraged the memorization effect (*i.e.* the phenomenon that difficult-to-learn patterns are typically memorized after easier ones) (Arpit et al., 2017). Building upon this observation, they introduced the Boosted Contrastive Learning (BCL) method, which emphasizes tail samples by employing more potent augmentation techniques.

Recently, Bai et al. (2023) explored utilizing external unlabeled OOD data to rebalance classes with rare samples. This

approach is motivated by the fact that acquiring additional ID data is expensive while valuable for balancing long-tailed datasets. Hence, they estimated tail samples and added samples from external data to ID dataset to rebalance the long-tail distribution during training.

2.2. Imbalanced Learning with Auxiliary Data

Jiang et al. (2021a) explored a method that samples additional data from an external source to enhance SSL on imbalanced datasets. They introduced a novel unlabeled data sampling framework, Model-Aware K-center (MAK). It is designed to sample additional diverse data for tail classes while preventing the inclusion of out-of-distribution outliers. While Jiang et al. (2021a) demonstrated its effectiveness in improving representation quality and balancedness, this method assumes the presence of ID data within the external sources.

Since acquiring additional ID data is expensive, researchers have investigated using external datasets containing only OOD data to enhance imbalanced learning. Wei et al. (2022) presented a method that assigns open-set noisy labels to OOD data to rebalance label distributions for long-tailed datasets. It then trains a network using the labels like supervised learning. As mentioned earlier, Bai et al. (2023) recently introduced a method that enhances SSL on long-tailed datasets using OOD data. Considering the ease of collecting unlabeled online data, researchers have also explored using auxiliary data in various tasks, such as anomaly detection (Hendrycks et al., 2019) and out-of-distribution data augmentation (Lee et al., 2021).

We investigate utilizing additional OOD data for self-supervised representation learning on long-tailed datasets similar to (Bai et al., 2023). Bai et al. (2023) trained a network using OOD and ID data and directly employed the network for downstream tasks. In contrast to the previous work, we pre-train a network using OOD and ID data and then further optimize the network using ID data and the pre-trained network. It is to learn an optimal embedding function for ID data while maintaining the balanced and well-separated embedding space from the frozen network. We experimentally verify the effectiveness of the proposed method by applying it to two existing works, SimCLR (Chen et al., 2020) and SDCLR (Jiang et al., 2021b). Different from (Jiang et al., 2021a), we do not assume the presence of ID data within an external dataset nor use any additional ID data, similar to (Wei et al., 2022; Bai et al., 2023).

2.3. Supervised Learning with Long-Tailed Datasets

Supervised long-tailed learning methods have been extensively studied including re-balancing, representation learning, and prompt tuning. For re-balancing, Park et al. (2022) introduced a minority over-sampling method that diversifies tail samples by pasting a tail sample onto an image from head classes. Later, Gao et al. (2023) proposed an adaptive image-mixing method to synthesize semantically more reasonable images for tail classes. Recently, Li et al. (2024a) proposed to augment samples from tail classes by replacing parts of their feature maps with those from head classes.

Instead of generating synthetic images for minority classes, Li et al. (2022) introduced the Gaussian clouded logit adjustment method which assigns larger margins to tail classes than to head classes to enhance the separability of tail classes. Later, Chen and Su (2023) presented a knowledge-transfer-based calibration method that estimates and utilizes importance weights for samples from rare classes. Another method, presented in (Jin et al., 2023), proposed a self-heterogeneous integration framework that adopts and improves mixture-of-experts strategies.

With the advent of pre-trained models on web-scale datasets, Dong et al. (2023) presented a prompt tuning method for long-tailed classification tasks. To enhance generalization performance on rare classes, Li et al. (2024b) proposed the Gaussian neighborhood minimization prompt tuning method for visual prompt tuning. Shi et al. (2024a) demonstrated that excessive fine-tuning of foundation models deteriorates performance on tail classes and introduced a lightweight fine-tuning method.

3. Proposed Method

To learn an optimal embedding space for a long-tailed dataset without any labels, we propose to first pre-train an embedding network using sampled out-of-distribution (OOD) data and in-domain (ID) data and then further optimize the network for the ID data by leveraging the pre-trained network, as presented in Figure 1.

Because most data in a long-tailed dataset belong to head classes, embedding networks trained using typical unsupervised contrastive learning methods tend to poorly represent samples belonging to tail classes. This results in limited performance in downstream tasks. To overcome this limitation, we leverage OOD data that are close to the tail samples to rebalance the data distribution for unsupervised contrastive learning, as presented in Section 3.1. The rebalanced data contribute to learning a more balanced and well-separated embedding space.

However, the learned embedding space using the rebalanced data might not be optimal for the target ID data. Additionally, the sampled OOD data for the tail classes might be noisy. Hence, to obtain an optimal embedding network for the ID data, we further train the network using the ID data and the pre-trained network, as described in Section 3.2. The pre-trained network is utilized to select proper positive/negative samples and to control strengths of attractive/repulsive forces. Additionally, the pre-trained network is employed to transfer its balanced and well-separated embedding space to the training network.

3.1. Unsupervised Contrastive Pre-training

We investigate unsupervised contrastive pre-training that leverages OOD data alongside long-tailed ID data to learn a more balanced embedding space. Additionally, we present a method that assigns pseudo semantic labels and encodes semantic relationships to enhance linear separability between samples of different classes. The pre-trained network is utilized to learn a further optimal embedding network for ID data in Section 3.2.

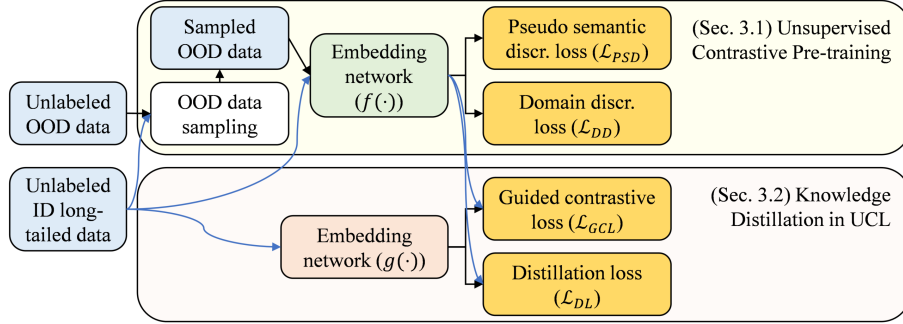


Figure 1: Overview of the proposed framework during training. In the unsupervised contrastive pre-training stage, an embedding network $f(\cdot)$ is trained using ID long-tailed data and sampled OOD data by back-propagating pseudo semantic discrimination loss \mathcal{L}_{PSD} and domain discrimination loss \mathcal{L}_{DD} . In the knowledge distillation stage, the final embedding network $g(\cdot)$ is trained using ID data and the pre-trained network $f(\cdot)$ by back-propagating guided contrastive loss \mathcal{L}_{GCL} and distillation loss \mathcal{L}_{DL} .

3.1.1. Sampling Out-Of-Domain Data

To learn a balanced embedding space for a long-tailed dataset, we sample additional images that seem to contain objects of tail classes from an out-of-distribution (OOD) dataset \mathcal{D}^{OOD} . To select OOD images that are closely related to tail classes, we first cluster the feature embeddings of in-domain (ID) images \mathcal{D}^{ID} into N_c clusters where each cluster is interpreted as a semantic class. We then compute a tailness score for each cluster, indicating the likelihood of containing objects of a tail class. Subsequently, we allocate a sampling budget to each cluster based on its tailness score. Finally, we sample OOD images that are close to the centroids of these clusters.

In-Domain Sample Clustering. To cluster the embeddings of long-tailed ID images, we adapt the Kullback–Leibler (KL) divergence-based clustering method in (Zhang et al., 2021). While Bai et al. (2023) utilized a standard k -means clustering algorithm, it tends to assign most cluster centroids near samples belonging to head classes, with only a few centers close to samples of tail classes. Consequently, it has limitations in grouping samples from tail classes, which in turn results in challenges in allocating sampling budgets and sampling OOD images for tail classes.

Given the entire ID images $\mathcal{D}^{ID} = \{\mathbf{I}_i\}_{i=1}^{N_{ID}}$, we first apply an embedding network $f(\cdot)$ to extract their feature embeddings $\mathcal{Z}^{ID} = \{\mathbf{z}_i\}_{i=1}^{N_{ID}}$ where $\mathbf{z}_i = f(\mathbf{I}_i)$. N_{ID} denotes the number of samples in \mathcal{D}^{ID} . We then initialize cluster centroids using cluster centers obtained by applying a standard k -means clustering algorithm to the feature embeddings \mathcal{Z}^{ID} . Subsequently, we refine the cluster centroids iteratively using the KL divergence-based clustering method.

To refine the centroids $\{\boldsymbol{\mu}_k\}_{k=1}^{N_c}$, we first perform a soft assignment of the feature embeddings \mathbf{z}_i to the clusters, where N_c denotes the number of clusters. Specifically, following (van der Maaten and Hinton, 2008), we employ Student’s t -distribution to estimate the probability q_{ik} that sample \mathbf{x}_i belongs to cluster k based on the distance between the sample’s embedding vector \mathbf{z}_i and the cluster center $\boldsymbol{\mu}_k$.

$$q_{ik} := \frac{(1 + \|\mathbf{z}_i - \boldsymbol{\mu}_k\|_2^2/d)^{-\frac{d+1}{2}}}{\sum_{k=1}^{N_c} (1 + \|\mathbf{z}_i - \boldsymbol{\mu}_k\|_2^2/d)^{-\frac{d+1}{2}}} \quad (1)$$

where d denotes the degree of freedom of the t -distribution. We set $d = 1$ following (Zhang et al., 2021) due to the absence of a validation set to search for this hyperparameter.

We then iteratively refine the centroids $\{\boldsymbol{\mu}_k\}_{k=1}^{N_c}$ by minimizing the KL divergence between the current soft assignment q_{ik} and the auxiliary target assignment probability, following (Xie et al., 2016). The target distribution p_{ik} is defined as follows:

$$p_{ik} := \frac{q_{ik}^2/h_k}{\sum_{k=1}^{N_c} q_{ik}^2/h_k} \quad \text{where} \quad h_k := \sum_{i=1}^B q_{ik}. \quad (2)$$

B represents the number of samples in a minibatch. h_k is the soft sample frequency for cluster k . Squaring of q_{ik} emphasizes reliance on highly confident samples while reducing the influence of samples with lower confidence. h_k normalizes to balance clusters with different sample counts.

Then, the KL divergence-based loss is computed as follows:

$$\mathcal{L}_{cluster} := \frac{1}{B} \sum_{i=1}^B \sum_{k=1}^{N_c} p_{ik} \log \frac{p_{ik}}{q_{ik}}. \quad (3)$$

The iterative refinement of $\boldsymbol{\mu}_k$ using $\mathcal{L}_{cluster}$ terminates when the proportion of samples with changed cluster assignments falls below a threshold. After termination, each sample \mathbf{x}_i is assigned to the closest cluster k based on the L2 distance between \mathbf{z}_i and $\boldsymbol{\mu}_k$.

Cluster-Wise Tailness Score Estimation. We compute the cluster-wise scores by first estimating the score of each ID sample belonging to tail classes and then averaging the scores of the samples within each cluster.

To estimate the tailness score for an instance \mathbf{x}_i , we first form a set \mathcal{Z}^i containing \mathbf{z}_i and its K nearest neighbors in the embedding space given $\mathcal{Z}^{ID} = \{\mathbf{z}_i\}_{i=1}^{N_{ID}}$. Subsequently, we compute the cosine similarities $s_{cos}(\mathbf{z}_i, \mathbf{z}_j)$ between all pairs of the samples in \mathcal{Z}^i . Since samples belonging to head classes tend to have higher densities in the embedding space than those of tail classes, we use the cosine similarities to estimate the density of each sample’s neighborhood and to compute its tailness score. Specifically, the score \hat{s}_i^t for sample \mathbf{x}_i is computed as follows:

$$\hat{s}_i^t := -\frac{\sum_{\mathbf{z}_m \in \mathcal{Z}^i} \sum_{\mathbf{z}_n \in (\mathcal{Z}^i \setminus \mathbf{z}_m)} \exp(s_{cos}(\mathbf{z}_m, \mathbf{z}_n))}{K(K+1)} \quad (4)$$

where t denotes the current epoch during training.

To enhance the robustness of the estimated scores, we apply momentum updates to them. Accordingly, the tailness score s_i^t for sample x_i is updated as follows:

$$s_i^t := \rho s_i^{(t-T)} + (1 - \rho) \hat{s}_i^t \quad (5)$$

where ρ represents the momentum hyperparameter with a value between 0 and 1. When $t = 0$, $s_i^0 = \hat{s}_i^0$. The score s_i^t is updated every T epochs for efficiency. A higher score s_i^t indicates that the corresponding sample x_i has a sparser neighborhood in the embedding space, implying a higher probability of belonging to tail classes.

Lastly, we compute the cluster-wise tailness score s_k^{tail} by averaging the instance-wise scores s_i^t of the samples within each cluster as follows:

$$s_k^{tail} := \frac{1}{|C_k|} \sum_{i \in C_k} s_i^t \quad (6)$$

where C_k denotes the set containing the sample indices in cluster k , and $|C_k|$ represents the number of samples in C_k . While Bai et al. (2023) estimated instance-wise tailness scores using only the samples in a minibatch, we compute them using the entire data for better accuracy and robustness.

Sampling Budget Allocation & OOD Data Sampling. We allocate more sampling budgets to the clusters with higher cluster-wise tailness scores s_k^{tail} . Following (Bai et al., 2023), the sampling budget u_k for cluster k is assigned as follows:

$$u_k := N_b \cdot S\left(\frac{\hat{s}_k^{tail}}{\tau}\right) \quad \text{where} \quad \hat{s}_k^{tail} := \frac{s_k^{tail} - \mu(s^{tail})}{\sigma(s^{tail})}. \quad (7)$$

N_b denotes the total sampling budget; $S(\cdot)$ represents a softmax function; \hat{s}_k^{tail} is the normalized cluster-wise tailness score; $\mu(\cdot)$ and $\sigma(\cdot)$ denote mean and standard deviation operations, respectively; τ represents the temperature hyperparameter.

Based on the allocated sampling budget for each cluster, we sample OOD images whose feature embeddings are close to the cluster center. We denote the set containing all N_b sampled OOD images as \mathcal{D}_s^{OOD} . We update the set \mathcal{D}_s^{OOD} every T epochs to deal with changes in the embedding space.

3.1.2. Pre-training With Sampled OOD Data

To enhance the separability of samples from different classes, we investigate a method that assigns pseudo semantic labels and encodes semantic relationships using both ID and sampled OOD data. Typical unsupervised contrastive learning (UCL) methods employ instance discrimination tasks to train an embedding network due to the absence of labels. Specifically, they use an augmented version of an instance as its positive sample and other instances as negative samples. Consequently, they also push apart instances from the same class. Therefore, we utilize the proximity of samples to encode semantic relationships. Moreover, the embedding network learns a more balanced embedding space by incorporating sampled OOD data into long-tailed ID data since instances in the merged dataset are more uniformly distributed in the embedding space.

In detail, we first sample an instance x_i from the merged dataset \mathcal{D} containing instances of both the ID dataset \mathcal{D}^{ID} and the sampled OOD dataset \mathcal{D}_s^{OOD} . We then find K^{pos} nearest neighbors based on cosine similarity in the embedding space. The nearest neighboring samples are considered as positive samples in addition to the instance’s augmented sample, while the other samples in a minibatch are used as negative samples. Subsequently, we train the embedding network to increase the similarities between the instance and positive samples while reducing the similarities between the instance and negative samples. Since we consider instance-wise nearest neighbors as samples with the same pseudo semantic class, we refer to the corresponding loss as the pseudo semantic discrimination loss. The loss \mathcal{L}_{PSD} is computed as follows:

$$\mathcal{L}_{PSD} := -\frac{1}{|\mathcal{Z}^B|} \sum_{z_i \in \mathcal{Z}^B} \log \frac{\sum_{z_j \in \mathcal{S}_i^{pos}} \exp(z_i \cdot z_j / \tau)}{\sum_{z_j \in \mathcal{S}_i^{neg}} \exp(z_i \cdot z_j / \tau)} \quad (8)$$

where \mathcal{Z}^B represents the set containing the embeddings of instances in the minibatch. \mathcal{S}_i^{pos} and \mathcal{S}_i^{neg} denote sets consisting of the embeddings of positive samples and negative samples of z_i , respectively. $|\mathcal{Z}^B|$ represents the number of samples in \mathcal{Z}^B . τ denotes the temperature hyperparameter. The nearest neighboring instances are selected among the samples within the instance’s domain (either ID or OOD). The nearest neighbors for each instance are updated every T epochs.

In addition to the pseudo semantic discrimination loss, we utilize the domain discrimination loss in (Bai et al., 2023). Unlike typical unsupervised contrastive learning, we use a combined dataset containing samples from two different domains and know the origin domain of each sample. Accordingly, the domain discrimination loss is computed using the domain information as ground-truth labels, which aims to bring samples from the same domain closer together while pushing those from different domains farther apart. The loss \mathcal{L}_{DD} is calculated as follows:

$$\mathcal{L}_{DD} := -\frac{1}{|\mathcal{Z}^B|} \sum_{z_i \in \mathcal{Z}^B} \frac{1}{|\mathcal{S}_i^s|} \sum_{z_p \in \mathcal{S}_i^s} \log \left(\frac{\exp(z_i \cdot z_p / \tau)}{\exp(z_i \cdot z_p / \tau) + \sum_{z_n \in \mathcal{S}_i^d} \exp(z_i \cdot z_n / \tau)} \right) \quad (9)$$

where \mathcal{Z}^B represents the set containing the embeddings of instances in the minibatch. \mathcal{S}_i^s and \mathcal{S}_i^d denote sets consisting of embeddings of samples within the same domain and those from the different domain compared to z_i , respectively. $|\mathcal{S}_i^s|$ represents the number of samples in \mathcal{S}_i^s .

The total contrastive pre-training loss \mathcal{L}_{CPT} is computed through a weighted summation of \mathcal{L}_{PSD} and \mathcal{L}_{DD} as follows:

$$\mathcal{L}_{CPT} := \mathcal{L}_{PSD} + \alpha \mathcal{L}_{DD} \quad (10)$$

where α is a hyperparameter used to balance the two losses.

3.2. Knowledge Distillation in UCL

The pre-trained embedding network in Section 3.1 encodes balanced embeddings with good separability between samples

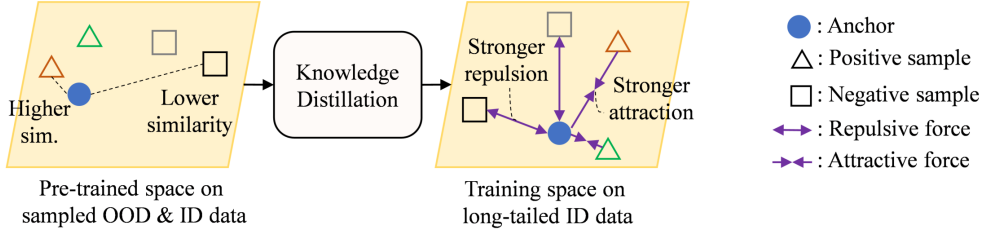


Figure 2: Proposed method leverages the balanced and well-separated embedding space of a pre-trained network to train a further optimal network for in-domain data. The pre-trained network is trained on out-of-distribution data and in-domain data.

of different classes by incorporating sampled OOD data and learning semantic and domain discriminations. However, the pre-trained network might not be optimal for the ID dataset. Therefore, we train a further optimal embedding network for the ID dataset while using the pre-trained network as a guiding network in unsupervised contrastive learning (UCL). We leverage the balanced and well-separated embedding space from the pre-trained network to select valid positive/negative samples and to control strengths of attractive/repulsive forces in contrastive learning, as presented in Figure 2. Additionally, we distil the embedding space from the pre-trained network and transfer it to the training network.

In detail, we first initialize a new embedding network $g(\cdot)$ using the pre-trained and frozen guiding network $f(\cdot)$. Subsequently, we further optimize the network $g(\cdot)$ using the ID dataset \mathcal{D}^{ID} and the guiding network $f(\cdot)$. To train $g(\cdot)$, we sample instances from \mathcal{D}^{ID} and extract their embeddings using the guiding network $f(\cdot)$. We then utilize the embeddings to select positive and negative samples since the guiding network is already capable of semantic discrimination. For each instance, a positive sample is randomly selected from the K^{kd} nearest neighbors in the embedding space, and a negative sample is randomly chosen among instances in the farthest cluster from the instance’s cluster. A cluster index is assigned to each ID data by applying the clustering method in Section 3.1 to the embeddings from the frozen network $f(\cdot)$.¹ Finally, we train the new network $g(\cdot)$ using the sampled instances and their positive/negative samples by minimizing the proposed guided contrastive loss and the distillation loss.

For the guided contrastive loss, given an instance x_i and its positive/negative samples (x_i^p, x_i^n) , we first extract embeddings (z_i, z_i^p, z_i^n) using the guiding network $f(\cdot)$ and embeddings (y_i, y_i^p, y_i^n) using the current embedding network $g(\cdot)$. Then, we compute the cosine similarity w_i^{pos} between z_i and z_i^p and the similarity w_i^{neg} between z_i and z_i^n . Subsequently, these similarities (w^{pos}, w^{neg}) are utilized as weighting coefficients in the guided contrastive loss. The coefficients control the strengths of attractive/repulsive forces in contrastive learning. Positive samples with higher w_i^{pos} are heavily pulled closer together, while negative samples with lower w_i^{neg} are strongly pushed farther apart. Consequently, the guided contrastive loss \mathcal{L}_{GCL} is com-

puted as follows:

$$\mathcal{L}_{GCL} := \frac{1}{|\mathcal{X}^B|} \sum_{i \in \mathcal{X}^B} \left[(1 + w_i^{pos})(1 - s_{cos}(y_i, y_i^p)) + (1 - w_i^{neg})(1 + s_{cos}(y_i, y_i^n)) \right] \quad (11)$$

where \mathcal{X}^B represents the set containing the indices of instances in the minibatch. $s_{cos}(\cdot, \cdot)$ denotes the cosine similarity function. $|\mathcal{X}^B|$ represents the number of samples in \mathcal{X}^B .

In addition to the guided contrastive loss, we employ a distillation loss to maintain the embedding structure of the guiding network in the new embedding network. The distillation loss is computed by comparing the cosine similarities from the guiding network $f(\cdot)$ to those from the current network $g(\cdot)$. Consequently, the loss is calculated as follows:

$$\mathcal{L}_{DL} := \frac{1}{|\mathcal{X}^B|(|\mathcal{X}^B| - 1)} \sum_{i \in \mathcal{X}^B} \sum_{j \in (\mathcal{X}^B \setminus i)} \left[(s_{cos}(z_i, z_j) - s_{cos}(y_i, y_j))^2 \right] \quad (12)$$

where \mathcal{X}^B represents the set containing the indices of instances in the minibatch.

The total guided learning loss is computed through a weighted summation of \mathcal{L}_{GCL} and \mathcal{L}_{DL} as follows:

$$\mathcal{L}_{GL} := \mathcal{L}_{GCL} + \beta \mathcal{L}_{DL} \quad (13)$$

where β is a hyperparameter used to balance the two losses.

4. Experiments and Results

4.1. Experimental Setting

Dataset. Experiments are conducted using four public long-tailed datasets: CIFAR-10-LT, CIFAR-100-LT, ImageNet-100-LT, and Places-LT, following previous work (Bai et al., 2023). CIFAR-10-LT and CIFAR-100-LT datasets (Cui et al., 2019) contain subsets of images from the original CIFAR-10 and CIFAR-100 datasets (Krizhevsky, 2009), respectively. The imbalance ratio of 100 is used. We utilize 300K Random Images from (Hendrycks et al., 2019) as the OOD dataset, following (Wei et al., 2022). ImageNet-100-LT (Jiang et al., 2021b) comprises 12K images sampled from ImageNet-100 (Tian et al., 2020) using a Pareto distribution. The number of instances for each class ranges from 5 to 1,280. ImageNet-R (Hendrycks et al., 2021) is used as the OOD dataset. Places-LT (Liu et al., 2019) consists of about 62.5K images sampled

¹Clustering is performed only once at the beginning due to the fixed embeddings from the frozen network.

Table 2: Quantitative comparison of accuracies and balancedness using the CIFAR-10-LT and CIFAR-100-LT datasets (Cui et al., 2019).

Dataset	Method	Many \uparrow	Med. \uparrow	Few \uparrow	STD \downarrow	All \uparrow
CIFAR	SimCLR (Chen et al., 2020)	82.40	73.91	70.19	5.11	75.34
	SimCLR + COLT (Bai et al., 2023)	87.50	81.65	80.80	2.98	83.15
	SimCLR + KDUP (ours)	93.80	89.17	87.36	2.71	90.26
-10-LT	SDCLR (Jiang et al., 2021b)	86.69	82.15	76.23	4.28	81.74
	SDCLR + COLT (Bai et al., 2023)	90.87	84.28	81.45	3.95	85.41
	SDCLR + KDUP (ours)	95.23	89.79	88.65	2.87	91.42
CIFAR	SimCLR (Chen et al., 2020)	51.50	45.58	45.96	2.71	47.65
	SimCLR + COLT (Bai et al., 2023)	57.94	56.74	57.72	0.52	57.46
	SimCLR + KDUP (ours)	63.83	62.47	61.96	0.79	62.36
-100-LT	SDCLR (Jiang et al., 2021b)	58.54	55.70	52.10	2.64	55.48
	SDCLR + COLT (Bai et al., 2023)	63.28	60.85	59.42	1.59	61.18
	SDCLR + KDUP (ours)	66.95	64.56	63.45	1.46	64.98

from Places dataset (Zhou et al., 2017) using a Pareto distribution. The number of instances for each class ranges from 5 to 4,980. We employ Places-Extra69 (Zhou et al., 2017) as the OOD dataset.

Evaluation Protocol. We employ two standard evaluation protocols: linear probing and few-shot learning. Initially, we train the embedding model $g(\cdot)$ with the proposed method using unlabeled data. Subsequently, we freeze the model $g(\cdot)$ and append a linear classifier to the frozen model. Finally, we train only the linear classifier, using the entire data with labels for linear probing and 1% of the labeled data for few-shot learning, respectively.

After training the linear classifier, we compute accuracies to evaluate the separability and balancedness of the learned embedding space. The overall accuracy is utilized to assess the linear separability. To measure its balancedness, we divide a test dataset into three disjoint groups (*i.e.* Many, Medium, Few) based on the number of instances for each class. Then, we assess the balancedness by calculating the standard deviation of the accuracies for these three groups.

Implementation Details. We apply the proposed method to SimCLR (Chen et al., 2020) and SDCLR (Jiang et al., 2021b) using ResNet-18 as the backbone for CIFAR-10-LT and CIFAR-100-LT datasets, following (Bai et al., 2023). For ImageNet-100-LT and Places-LT datasets, the proposed method is applied to SimCLR (Chen et al., 2020) with ResNet-50 as the backbone.

We pre-train the networks for 2,000, 2,000, 1,000, and 500 epochs for the CIFAR-10-LT, CIFAR-100-LT, ImageNet-100-LT, and Places-LT datasets, respectively, using the method in Section 3.1. We then further optimize the networks for 500 epochs for all datasets using the method in Section 3.2. Lastly, for evaluation, we train the linear classifier for 30 epochs and 100 epochs for linear probing and few-shot learning protocols, respectively, for all datasets. T is set to 50 epochs for the ImageNet-100-LT dataset and 25 epochs for all the other datasets. In Section 3.1, $K = 10$, $\rho = 0.9$, $N_b = 10,000$, $K^{pos} = 3$, and $\alpha = 0.3$. In Section 3.2, $K^{kd} = 5$ and $\beta = 0.4$.

The code will be made available on GitHub upon publication to ensure better reproducibility.

4.2. Result

We present quantitative results of the proposed method and previous works on the CIFAR-10-LT and CIFAR-100-LT datasets (Cui et al., 2019) in Table 2. Following (Bai et al., 2023), linear probing is utilized for evaluation. For the CIFAR-10-LT dataset, the proposed method outperforms COLT (Bai et al., 2023) by 7.11% and 6.01% in overall accuracy with 0.27 and 1.08 lower standard deviation (STD) when integrated with SimCLR (Chen et al., 2020) and SDCLR (Jiang et al., 2021b), respectively. For the CIFAR-100-LT dataset, the proposed framework achieves 4.9% and 3.8% higher overall accuracies with 0.27 higher and 0.13 lower STD compared to COLT (Bai et al., 2023) with SimCLR (Chen et al., 2020) and SDCLR (Jiang et al., 2021b), respectively. While the higher STD of the proposed method with SimCLR represents lower balancedness compared with the previous work, it is worth noting that our absolute STD value is only 0.79, which is still very low.

Table 3 shows quantitative comparisons of the proposed method with previous works on the ImageNet-100-LT (Jiang et al., 2021b) and Places-LT (Liu et al., 2019) datasets. All methods in this table are implemented on top of SimCLR (Chen et al., 2020) and evaluated using both linear probing and few-shot learning protocols. The proposed method consistently outperforms the previous state-of-the-art method for all datasets and protocols by achieving higher accuracies and lower STDs. For the ImageNet-100-LT dataset, the proposed method achieves 1.61% and 2.19% higher overall accuracies with 0.12 and 0.19 lower STDs than SimCLR+COLT (Bai et al., 2023) in few-shot learning and linear probing, respectively. For the Places-LT dataset, the proposed framework outperforms SimCLR+COLT (Bai et al., 2023) by 0.76% and 1.45% in overall accuracies with 0.11 and 0.22 lower STDs in few-shot learning and linear probing, respectively.

Table 3: Quantitative comparison of accuracies and balancedness using the ImageNet-100-LT (Jiang et al., 2021b) and Places-LT datasets (Liu et al., 2019).

Dataset	Protocol	Method	Many \uparrow	Med. \uparrow	Few \uparrow	STD \downarrow	All \uparrow
ImageNet -100-LT	Few -shot	Random sampling	52.82	42.88	40.27	5.41	46.42
		MAK (Jiang et al., 2021a)	54.33	45.01	40.12	5.90	48.01
		COLT (Bai et al., 2023)	54.26	46.54	43.38	4.57	49.14
		KDUP (ours)	56.08	48.41	45.59	4.45	50.75
	Linear -probing	Random sampling	74.33	68.52	62.65	4.77	70.02
		MAK (Jiang et al., 2021a)	75.57	68.20	66.29	4.07	70.83
		COLT (Bai et al., 2023)	75.13	71.38	66.62	3.48	72.22
		KDUP (ours)	77.91	74.07	69.84	3.29	74.41
Places -LT	Few- shot	Random sampling	30.61	33.94	37.55	2.83	33.45
		MAK (Jiang et al., 2021a)	30.41	34.47	37.59	2.94	33.62
		COLT (Bai et al., 2023)	31.04	34.65	37.49	2.64	33.91
		KDUP (ours)	31.85	35.31	38.02	2.53	34.67
	Linear -probing	Random sampling	40.21	47.59	50.51	4.33	45.51
		MAK (Jiang et al., 2021a)	40.83	47.78	50.72	4.15	45.86
		COLT (Bai et al., 2023)	41.55	48.40	50.54	3.83	46.36
		KDUP (ours)	43.18	49.74	51.61	3.61	47.81

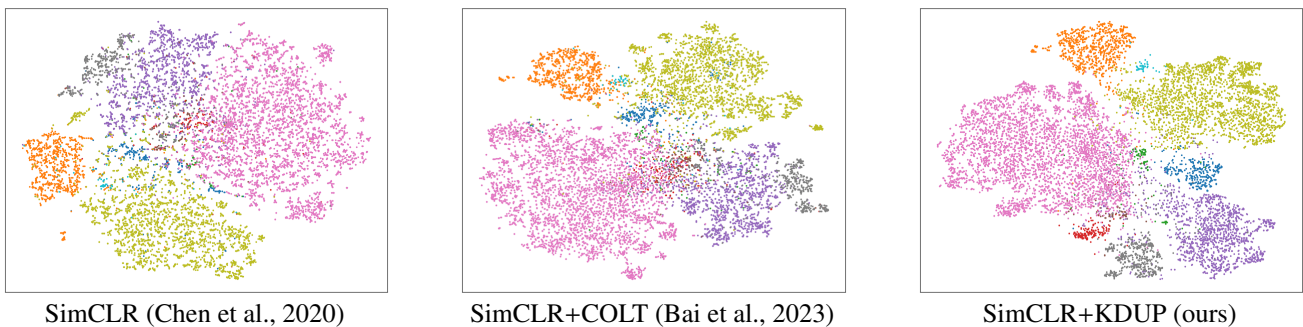


Figure 3: t-SNE visualization of the CIFAR-10-LT dataset (Cui et al., 2019).

Figure 3 visualizes a t-SNE projection of the learned representations of the data in the CIFAR-10-LT dataset (Cui et al., 2019). This figure demonstrates that the proposed method has better separability between samples of different classes and forms more compact clusters for each class than previous works (Chen et al., 2020; Bai et al., 2023).

Additionally, in Table 4, we quantitatively compare the learned representations of the proposed method with those of the previous state-of-the-art method, COLT (Bai et al., 2023), using the Calinski-Harabasz Index (CHI) (Caliński and Harabasz, 1974) and the Davies-Bouldin Index (DBI) (Davies and Bouldin, 1979). All the scores in the table are computed using the models based on SimCLR (Chen et al., 2020). In addition to the results shown in Figure 3, the measured CHI and DBI scores demonstrate that the proposed method forms more compact clusters for each class while achieving better separation between different classes than the previous work.

4.3. Analysis

We present an ablation study of the proposed framework using the CIFAR-10-LT dataset (Cui et al., 2019) in Table 5.

The experiments are conducted with models based on SimCLR (Chen et al., 2020) and the linear probing protocol. Firstly, we construct a strong baseline model by incorporating the KL divergence-based clustering method instead of k -means clustering and the proposed tailness score estimation. The baseline model achieves 1.56% higher accuracy and 0.10 lower STD than SimCLR+COLT (Bai et al., 2023). By employing the proposed pseudo semantic discrimination method, we further enhance overall accuracy by 3.74% with 0.08 lower STD. Finally, the proposed knowledge distillation method in Section 3.2 further improves overall accuracy by 1.81% with 0.09 lower STD. Additionally, we present the results of the strong baseline model excluding the domain discrimination loss \mathcal{L}_{DD} ².

Table 6 presents a detailed analysis of the guided contrastive loss \mathcal{L}_{GCL} using the models based on SimCLR (Chen et al., 2020), the linear probing protocol, and the CIFAR-10-LT dataset (Cui et al., 2019). The top row shows the results of our method without the knowledge distillation (KD) stage

²Please note that COLT (Bai et al., 2023) also employs the domain discrimination loss \mathcal{L}_{DD} .

Table 4: Quantitative comparison of the learned representations using the Calinski-Harabasz Index (CHI) and the Davies-Bouldin Index (DBI) on the CIFAR-10-LT, CIFAR-100-LT, ImageNet-100-LT, and Places-LT datasets.

Dataset	Method	CHI \uparrow	DBI \downarrow
CIFAR-10-LT	COLT (Bai et al., 2023)	143.62	3.38
	KDUP (ours)	187.03	2.21
CIFAR-100-LT	COLT (Bai et al., 2023)	103.47	4.25
	KDUP (ours)	132.58	3.64
ImageNet-100-LT	COLT (Bai et al., 2023)	121.63	3.79
	KDUP (ours)	155.74	2.85
Places-LT	COLT (Bai et al., 2023)	89.82	5.83
	KDUP (ours)	102.71	4.97

Table 5: Ablation study of the proposed method on the CIFAR-10-LT dataset (Cui et al., 2019).

Method	Many \uparrow	Medium \uparrow	Few \uparrow	STD \downarrow	All \uparrow
SimCLR (Chen et al., 2020)	82.40	73.91	70.19	5.11	75.34
Strong Baseline w/o \mathcal{L}_{DD}	87.31	81.79	80.24	3.67	83.25
Strong Baseline	88.93	83.07	82.59	2.88	84.71
+ Semantic Discrimination \mathcal{L}_{PSD}	92.06	87.82	85.27	2.80	88.45
+ Knowledge Distillation \mathcal{L}_{GL}	93.80	89.17	87.36	2.71	90.26

Table 6: Analysis of the proposed guided contrastive loss \mathcal{L}_{GCL} .

Method	Many \uparrow	Medium \uparrow	Few \uparrow	STD \downarrow	All \uparrow
Ours w/o KD (Sec. 3.2)	92.06	87.82	85.27	2.80	88.45
+ KD with typical loss	87.65	81.76	80.93	2.99	83.32
+ Guided Sampling	92.81	88.67	86.05	2.78	89.19
+ Guided Weighting	93.80	89.17	87.36	2.71	90.26

Table 7: Effectiveness of the proposed method under the experimental setting of MAK (Jiang et al., 2021a).

Method	Many \uparrow	Med. \uparrow	Few \uparrow	STD \downarrow	All \uparrow
MAK (Jiang et al., 2021a)	74.7 \pm 0.2	69.2 \pm 0.7	66.6 \pm 0.7	3.3 \pm 0.3	71.1 \pm 0.5
+ Semantic Discrimination \mathcal{L}_{PSD}	75.8 \pm 0.4	70.9 \pm 0.5	68.5 \pm 0.8	3.0 \pm 0.5	72.8 \pm 0.4
+ Knowledge Distillation \mathcal{L}_{GL}	76.3\pm0.3	72.1\pm0.5	69.1\pm0.6	2.9\pm0.4	73.4\pm0.3

in Section 3.2. The second row presents the results of employing a KD stage that uses a typical contrastive loss and \mathcal{L}_{DL} . Because the typical contrastive loss utilizes a random sample within a mini-batch as a negative sample, this naive implementation deteriorates the overall accuracy by 5.13%. Utilizing the pre-trained network for selecting positive/negative samples enhances the accuracy by 5.87% and 0.74% compared to the second and the first rows, respectively. Subsequently, controlling the strengths of attractive/repulsive forces further improves the accuracy by 1.04%.

Additionally, Table 7 demonstrates the effectiveness of the proposed method using the experimental setting of (Jiang et al., 2021a), which assumes the presence of both ID and OOD data in an external dataset. Following (Jiang et al., 2021a), we experiment on the ImageNet-100-LT dataset while using the ImageNet-Places-Mix (IPM) as the external dataset. The

IPM dataset utilizes 200 randomly sampled classes from the ImageNet-900 dataset for ID data and the Places dataset for OOD data. The experiments are conducted with models based on MAK (Jiang et al., 2021a) and the linear probing protocol. Firstly, by incorporating the proposed pseudo semantic discrimination into MAK (Jiang et al., 2021a), the overall accuracy is improved by 1.7% with 0.3 lower STD. The proposed knowledge distillation method in Section 3.2 further enhances overall accuracy by 0.6% with 0.1 lower STD. These experimental results verify that the proposed method is also effective in scenarios where an external dataset contains both ID and OOD data.

Table 8 presents an analysis of the hyperparameters in the loss functions \mathcal{L}_{CPT} and \mathcal{L}_{GL} using the proposed method based on SimCLR (Chen et al., 2020) and the CIFAR-10-LT dataset (Cui et al., 2019). The results indicate that the proposed method consistently outperforms previous works (Chen et al.,

Table 8: Analysis of the hyperparameters in \mathcal{L}_{CPT} and \mathcal{L}_{GL} using our method with SimCLR (Chen et al., 2020) on the CIFAR-10-LT dataset (Cui et al., 2019).

α	β	Many \uparrow	Medium \uparrow	Few \uparrow	STD \downarrow	All \uparrow
0.2	0.3	92.41	86.95	85.92	2.84	88.53
0.2	0.4	92.67	87.96	86.03	2.79	88.98
0.2	0.5	91.16	86.07	84.41	2.87	87.31
0.3	0.3	93.21	88.54	86.65	2.76	89.54
0.3	0.4	93.80	89.17	87.36	2.71	90.26
0.3	0.5	92.79	88.13	86.27	2.74	89.15
0.4	0.3	92.63	87.54	86.12	2.79	88.87
0.4	0.4	92.68	88.05	86.13	2.75	89.01
0.4	0.5	91.63	86.72	84.93	2.83	87.84

Table 9: Analysis of total OOD data sampling budget N_b using the CIFAR-10-LT dataset (Cui et al., 2019).

N_b	5K	10K	15K	20K
All \uparrow	88.13	90.26	89.41	87.65

Table 10: Analysis of OOD data sampling frequency T using the CIFAR-10-LT dataset (Cui et al., 2019).

T	10	25	50	100
All \uparrow	89.25	90.26	88.73	87.41

2020; Jiang et al., 2021b; Bai et al., 2023), even with suboptimal hyperparameter values.

We present the effects of varying N_b and T in Tables 9 and 10, respectively. The results demonstrate that our method based on SimCLR (Chen et al., 2020) consistently outperforms the previous SOTA method, SimCLR (Chen et al., 2020) + COLT (Bai et al., 2023), which achieves 83.15 with $N_b = 10\text{K}$ and $T = 25$.

In Table 11, we compare the proposed method with its variant that excludes the momentum updates for instance-wise tailness scores in Eq. (5). The experimental results demonstrate the effectiveness of the momentum updates in tailness score estimation, especially for tail classes. We believe this is because samples belonging to tail classes are sparser than those of head classes in the embedding space, resulting in noisier tailness score estimates for tail samples. Accordingly, the momentum updates lead to greater improvements for tail classes.

In Table 12, we compare the results of the proposed method with those obtained using augmented data in place of OOD data. For the CIFAR-10-LT and CIFAR-100-LT datasets, the proposed method samples images from the 300K Random Images dataset for each cluster, based on the sampling budget described in Section 3.1.1. In contrast, the augmentation-based method balances the number of images in each cluster by synthesizing images through typical data augmentation techniques. Specifically, three operations are randomly selected from the following five techniques: horizontal flip, crop, rotation, color jitter, and Gaussian blur. The experimental results demonstrate the advantages of using OOD data compared to in-domain augmented images.

We report the training time of our method based on SimCLR (Chen et al., 2020) for an epoch in Table 13, measured on a computer with two Nvidia GeForce RTX 2080 Ti GPUs and an Intel Core i9-10940X CPU. We report the processing time for updating an OOD sample set \mathcal{D}_s^{OOD} separately in Table 14 because sampling is only processed every 50 epochs for the ImageNet-100-LT dataset and every 25 epochs for all other datasets. This includes ID sample clustering, tailness estimation, budget allocation, and sampling. Because we use a fixed total sampling budget ($N_b = 10,000$) for all datasets regardless of the size of OOD datasets, a larger OOD dataset only increases the time for OOD data sampling while not affecting the time for other processing. Based on these reported times, the total training time for the CIFAR-10-LT dataset is calculated as follows: 9.65 (seconds/update) \times 2000 (epochs) / 25 (epochs/update) + 4.32 (seconds/epoch) \times 2000 (epochs) + 2.32 (seconds/epoch) \times 500 (epochs), which is approximately 2.94 hours.

Additionally, we show the detailed processing time for updating \mathcal{D}_s^{OOD} in Table 15. The time is measured using the CIFAR-10-LT dataset (Cui et al., 2019) as the ID dataset and the 300K Random dataset (Hendrycks et al., 2019) as the OOD dataset. Note that the rightmost column of Table 15 is the same as that of Table 14.

5. CONCLUSION

Towards robust self-supervised learning on long-tailed datasets, we present a novel method that pre-trains a network on ID and OOD data and further optimizes the network for an ID dataset. We propose to leverage the pre-trained network to discover positive/negative samples and control the strengths of attractive/repulsive forces in contrastive learning. Additionally, to maintain the balanced and well-separated embedding space from the pre-trained network, we propose to distill the embedding space and transfer to the training network. Moreover, during pre-training on ID and OOD data, we propose to assign pseudo semantic labels and encode semantic relationships to learn a balanced and well-separated embedding space. Lastly, we evaluate the proposed method using linear probing and few-shot learning protocols on four public datasets. The results demonstrate that our method outperforms previous state-of-the-art methods.

Table 11: Ablation study on the effectiveness of the momentum updates (MU) in Eq. (5) using the CIFAR-10-LT dataset (Cui et al., 2019).

Method	Many \uparrow	Medium \uparrow	Few \uparrow	STD \downarrow	All \uparrow
without MU	93.04	89.97	85.74	2.94	89.13
with MU	93.80	89.17	87.36	2.71	90.26

Table 12: Comparison of using augmented data and OOD data for constructing \mathcal{D}_s^{OOD} on the CIFAR-10-LT and CIFAR-100-LT datasets (Cui et al., 2019).

Dataset	\mathcal{D}_s^{OOD}	Many \uparrow	Medium \uparrow	Few \uparrow	STD \downarrow	All \uparrow
CIFAR-10-LT	augmented	89.74	86.32	82.05	3.14	86.18
	OOD	93.80	89.17	87.36	2.71	90.26
CIFAR-100-LT	augmented	61.03	59.81	58.37	1.12	59.74
	OOD	63.83	62.47	61.96	0.79	62.36

Table 13: Analysis of the training time for an epoch in seconds.

ID Dataset	Pre-train (Sec. 3.1)	Distillation (Sec. 3.2)
CIFAR-10-LT	4.32	2.32
CIFAR-100-LT	3.87	1.98
ImageNet-100-LT	11.25	6.82
Places-LT	37.84	33.12

Table 14: Analysis of the time for updating \mathcal{D}_s^{OOD} in seconds. The CIFAR-10-LT dataset is utilized as the ID dataset.

OOD Dataset (Size)	OOD Sampling (Sec. 3.1)
300K Random (300K)	9.65
ImageNet-R (12K)	1.07
Places-Extra69 (62.5K)	3.24

Acknowledgments

This work was supported by the Korea Evaluation Institute of Industrial Technology (KEIT) Grant through the Korea Government (MOTIE) under Grant 20018635.

References

- Akrim, A., Gogu, C., Vingerhoeds, R., Salaün, M., 2023. Self-supervised learning for data scarcity in a fatigue damage prognostic problem. *Engineering Applications of Artificial Intelligence* 120, 105837. URL: <https://www.sciencedirect.com/science/article/pii/S0952197623000210>, doi:<https://doi.org/10.1016/j.engappai.2023.105837>.
- Arpit, D., Jastrzebski, S., Ballas, N., Krueger, D., Bengio, E., Kanwal, M.S., Maharaj, T., Fischer, A., Courville, A., Bengio, Y., Lacoste-Julien, S., 2017. A closer look at memorization in deep networks, in: Precup, D., Teh, Y.W. (Eds.), *Proceedings of the 34th International Conference on Machine Learning*, PMLR. pp. 233–242. URL: <https://proceedings.mlr.press/v70/arpit17a.html>.
- Bai, J., Liu, Z., Wang, H., Hao, J., Feng, Y., Chu, H., Hu, H., 2023. On the effectiveness of out-of-distribution data in self-supervised long-tail learning, in: *International Conference on Learning Representations*. URL: <https://openreview.net/forum?id=v8JlQdiN9Sh>.
- Biswas, M., Buckchash, H., Prasad, D.K., 2024. pnnclr: Stochastic pseudo neighborhoods for contrastive learning based unsupervised representation learning problems. *Neurocomputing* 593, 127810. URL: <https://www.sciencedirect.com/science/article/pii/S0925231224005812>, doi:<https://doi.org/10.1016/j.neucom.2024.127810>.
- Calinski, T., Harabasz, J., 1974. A dendrite method for cluster analysis. *Communications in Statistics* 3, 1–27. doi:10.1080/03610927408827101.
- Chai, A.Y.H., Lee, S.H., Tay, F.S., Bonnet, P., Joly, A., 2024. Beyond supervision: Harnessing self-supervised learning in unseen plant disease recognition. *Neurocomputing* 610, 128608. URL: <https://www.sciencedirect.com/science/article/pii/S0925231224013791>, doi:<https://doi.org/10.1016/j.neucom.2024.128608>.
- Chawla, N.V., Bowyer, K.W., Hall, L.O., Kegelmeyer, W.P., 2002. Smote: synthetic minority over-sampling technique. *Journal of Artificial Intelligence Research* 16, 321–357.
- Chen, J., Su, B., 2023. Transfer knowledge from head to tail: Uncertainty calibration under long-tailed distribution, in: *2023 IEEE/CVF Conference on Computer Vision and Pattern Recognition (CVPR)*, pp. 19978–19987. doi:10.1109/CVPR52729.2023.01913.
- Chen, T., Kornblith, S., Norouzi, M., Hinton, G., 2020. A simple framework for contrastive learning of visual representations, in: III, H.D., Singh, A. (Eds.), *Proceedings of the 37th International Conference on Machine Learning*, PMLR. pp. 1597–1607. URL: <https://proceedings.mlr.press/v119/chen20j.html>.
- Cui, Y., Jia, M., Lin, T.Y., Song, Y., Belongie, S., 2019. Class-balanced loss based on effective number of samples, in: *Proceedings of the IEEE/CVF Conference on Computer Vision and Pattern Recognition*, pp. 9268–9277.
- Davies, D.L., Boulton, D.W., 1979. A cluster separation measure. *IEEE Transactions on Pattern Analysis and Machine Intelligence PAMI-1*, 224–227. doi:10.1109/TPAMI.1979.4766909.
- Dong, B., Zhou, P., YAN, S., Zuo, W., 2023. LPT: Long-tailed prompt tuning for image classification, in: *The Eleventh International Conference on Learning Representations*. URL: <https://openreview.net/forum?id=8p0VAeo8ie>.
- Drummond, C., Holte, R.C., 2003. C4.5, class imbalance, and cost sensitivity: Why under-sampling beats over-sampling, in: *ICML Workshops*.
- Fan, S., Zhang, X., Song, Z., Shao, W., 2022. Cumulative dual-branch network framework for long-tailed multi-class classification. *Engineering Applications of Artificial Intelligence* 114, 105080. URL: <https://www.sciencedirect.com/science/article/pii/S0952197622002329>, doi:<https://doi.org/10.1016/j.engappai.2022.105080>.
- Foret, P., Kleiner, A., Mobahi, H., Neyshabur, B., 2021. Sharpness-aware minimization for efficiently improving generalization, in: *International Conference on Learning Representations*. URL: <https://openreview.net/forum?id=6Tmlmposlrm>.
- Gao, J., Zhao, H., Li, Z., Guo, D., 2023. Enhancing minority classes by mixing: An adaptive optimal transport approach for long-tailed classification, in: Oh, A., Naumann, T., Globerson, A., Saenko, K., Hardt, M., Levine, S. (Eds.), *Advances in Neural Information Processing Systems*, Curran Associates, Inc. pp. 60329–60348. URL: https://proceedings.neurips.cc/paper_files/paper/2023/file/

Table 15: Measured time for updating \mathcal{D}_s^{OOD} in seconds. The CIFAR-10-LT (Cui et al., 2019) dataset is utilized as the ID dataset, and the 300K Random (Hendrycks et al., 2019) dataset is used as the OOD dataset.

Processing for updating \mathcal{D}_s^{OOD} (Sec. 3.1)	Clustering	Tailness estimation	Sampling	Total
Time	0.85	0.06	8.74	9.65

- bdabb5d4262bcfb6a1d529d690a6c82b-Paper-Conference.pdf.
- Gidaris, S., Singh, P., Komodakis, N., 2018. Unsupervised representation learning by predicting image rotations, in: International Conference on Learning Representations. URL: <https://openreview.net/forum?id=S1v4N210->.
- He, K., Fan, H., Wu, Y., Xie, S., Girshick, R., 2020. Momentum contrast for unsupervised visual representation learning, in: 2020 IEEE/CVF Conference on Computer Vision and Pattern Recognition (CVPR), pp. 9726–9735. doi:10.1109/CVPR42600.2020.00975.
- Hendrycks, D., Basart, S., Mu, N., Kadavath, S., Wang, F., Dorundo, E., Desai, R., Zhu, T., Parajuli, S., Guo, M., et al., 2021. The many faces of robustness: A critical analysis of out-of-distribution generalization, in: Proceedings of the IEEE/CVF International Conference on Computer Vision, pp. 8340–8349.
- Hendrycks, D., Mazeika, M., Dietterich, T., 2019. Deep anomaly detection with outlier exposure, in: International Conference on Learning Representations. URL: <https://openreview.net/forum?id=HyxCxhRcY7>.
- Japkowicz, N., Stephen, S., 2002. The class imbalance problem: A systematic study. *Intell. Data Anal.* 6, 429–449.
- Jiang, Z., Chen, T., Chen, T., Wang, Z., 2021a. Improving contrastive learning on imbalanced data via open-world sampling, in: Ranzato, M., Beygelzimer, A., Dauphin, Y., Liang, P., Vaughan, J.W. (Eds.), *Advances in Neural Information Processing Systems*, Curran Associates, Inc., pp. 5997–6009.
- Jiang, Z., Chen, T., Mortazavi, B.J., Wang, Z., 2021b. Self-damaging contrastive learning, in: Meila, M., Zhang, T. (Eds.), *Proceedings of the 38th International Conference on Machine Learning*, PMLR, pp. 4927–4939. URL: <https://proceedings.mlr.press/v139/jiang21a.html>.
- Jin, Y., Li, M., Lu, Y., Cheung, Y.m., Wang, H., 2023. Long-tailed visual recognition via self-heterogeneous integration with knowledge excavation, in: 2023 IEEE/CVF Conference on Computer Vision and Pattern Recognition (CVPR), pp. 23695–23704. doi:10.1109/CVPR52729.2023.02269.
- Krizhevsky, A., 2009. Learning multiple layers of features from tiny images. Citeseer URL: <https://www.cs.toronto.edu/~kriz/learning-features-2009-TR.pdf>.
- Lee, S., Park, C., Lee, H., Yi, J., Lee, J., Yoon, S., 2021. Removing undesirable feature contributions using out-of-distribution data, in: International Conference on Learning Representations. URL: <https://openreview.net/forum?id=eIHYL6fpbkA>.
- Li, M., Cheung, Y.M., Lu, Y., 2022. Long-tailed visual recognition via gaussian clouded logit adjustment, in: 2022 IEEE/CVF Conference on Computer Vision and Pattern Recognition (CVPR), pp. 6919–6928. doi:10.1109/CVPR52688.2022.00680.
- Li, M., Hu, Z., Lu, Y., Lan, W., Cheung, Y.m., Huang, H., 2024a. Feature fusion from head to tail for long-tailed visual recognition. *Proceedings of the AAAI Conference on Artificial Intelligence* 38, 13581–13589. URL: <https://ojs.aaai.org/index.php/AAAI/article/view/29262>, doi:10.1609/aaai.v38i12.29262.
- Li, M., Liu, Y., Lu, Y., Zhang, Y., Cheung, Y.m., Huang, H., 2024b. Improving visual prompt tuning by gaussian neighborhood minimization for long-tailed visual recognition, in: Globerson, A., Mackey, L., Belgrave, D., Fan, A., Paquet, U., Tomczak, J., Zhang, C. (Eds.), *Advances in Neural Information Processing Systems*, Curran Associates, Inc., pp. 103985–104009. URL: https://proceedings.neurips.cc/paper_files/paper/2024/file/bc667ac84ef58f2b5022da97a465cbab-Paper-Conference.pdf.
- Liu, H., HaoChen, J.Z., Gaidon, A., Ma, T., 2022. Self-supervised learning is more robust to dataset imbalance, in: International Conference on Learning Representations. URL: <https://openreview.net/forum?id=4AZz9osqrar>.
- Liu, X., Zhang, F., Hou, Z., Mian, L., Wang, Z., Zhang, J., Tang, J., 2023. Self-supervised learning: Generative or contrastive. *IEEE Transactions on Knowledge and Data Engineering* 35, 857–876. doi:10.1109/TKDE.2021.3090866.
- Liu, Z., Miao, Z., Zhan, X., Wang, J., Gong, B., Yu, S.X., 2019. Large-scale long-tailed recognition in an open world, in: Proceedings of the IEEE/CVF Conference on Computer Vision and Pattern Recognition, pp. 2537–2546.
- Logacjov, A., Bach, K., 2024. Self-supervised learning with randomized cross-sensor masked reconstruction for human activity recognition. *Engineering Applications of Artificial Intelligence* 128, 107478. URL: <https://www.sciencedirect.com/science/article/pii/S0952197623016627>, doi:<https://doi.org/10.1016/j.engappai.2023.107478>.
- Lu, X., Ye, X., Cheng, Y., 2024. An overlapping minimization-based oversampling algorithm for binary imbalanced classification. *Engineering Applications of Artificial Intelligence* 133, 108107. URL: <https://www.sciencedirect.com/science/article/pii/S0952197624002653>, doi:<https://doi.org/10.1016/j.engappai.2024.108107>.
- van der Maaten, L., Hinton, G., 2008. Visualizing data using t-sne. *Journal of Machine Learning Research* 9, 2579–2605. URL: <http://jmlr.org/papers/v9/vandermaaten08a.html>.
- Pang, S., Wang, W., Zhang, R., Hao, W., 2023. Hierarchical block aggregation network for long-tailed visual recognition. *Neurocomputing* 549, 126463. URL: <https://www.sciencedirect.com/science/article/pii/S0925231223005866>, doi:<https://doi.org/10.1016/j.neucom.2023.126463>.
- Park, S., Hong, Y., Heo, B., Yun, S., Choi, J.Y., 2022. The majority can help the minority: Context-rich minority oversampling for long-tailed classification, in: 2022 IEEE/CVF Conference on Computer Vision and Pattern Recognition (CVPR), pp. 6877–6886. doi:10.1109/CVPR52688.2022.00676.
- Shi, J.X., Wei, T., Zhou, Z., Shao, J.J., Han, X.Y., Li, Y.F., 2024a. Long-tail learning with foundation model: Heavy fine-tuning hurts, in: Salakhutdinov, R., Kolter, Z., Heller, K., Weller, A., Oliver, N., Scarlett, J., Berkenkamp, F. (Eds.), *Proceedings of the 41st International Conference on Machine Learning*, PMLR, pp. 45014–45039. URL: <https://proceedings.mlr.press/v235/shi24g.html>.
- Shi, S., Wang, P., Zhang, X., Fan, J., 2024b. Mitigating biases in long-tailed recognition via semantic-guided feature transfer. *Neurocomputing* 590, 127735. URL: <https://www.sciencedirect.com/science/article/pii/S092523122400506X>, doi:<https://doi.org/10.1016/j.neucom.2024.127735>.
- Tian, Y., Hénaff, O.J., Oord, A.v.d., 2021. Divide and contrast: Self-supervised learning from uncurated data, in: 2021 IEEE/CVF International Conference on Computer Vision (ICCV), pp. 10043–10054. doi:10.1109/ICCV48922.2021.00991.
- Tian, Y., Krishnan, D., Isola, P., 2020. Contrastive multiview coding, in: *Computer Vision—ECCV 2020: 16th European Conference, Glasgow, UK, August 23–28, 2020, Proceedings, Part XI 16*, Springer, pp. 776–794.
- Wang, Y., Zhai, J., 2024. Feature balanced re-enhanced network with multi-factor margin loss for long-tailed visual recognition. *Neurocomputing* 610, 128530. URL: <https://www.sciencedirect.com/science/article/pii/S0925231224013018>, doi:<https://doi.org/10.1016/j.neucom.2024.128530>.
- Wei, H., Tao, L., Xie, R., Feng, L., An, B., 2022. Open-sampling: Exploring out-of-distribution data for re-balancing long-tailed datasets, in: Chaudhuri, K., Jegelka, S., Song, L., Szepesvari, C., Niu, G., Sabato, S. (Eds.), *Proceedings of the 39th International Conference on Machine Learning*, PMLR, pp. 23615–23630. URL: <https://proceedings.mlr.press/v162/wei22c.html>.
- Wen, Z., Pizarro, O., Williams, S., 2025. Active self-semi-supervised learning for few labeled samples. *Neurocomputing* 614, 128772. URL: <https://www.sciencedirect.com/science/article/pii/S0925231224015431>, doi:<https://doi.org/10.1016/j.neucom.2024.128772>.
- Xiang, X., Zhang, Z., Chen, X., 2024. Curricular-balanced long-tailed learning. *Neurocomputing* 571, 127121. URL: <https://www.sciencedirect.com/science/article/pii/S0925231224015431>.

- com/science/article/pii/S0925231223012444, doi:<https://doi.org/10.1016/j.neucom.2023.127121>.
- Xie, J., Girshick, R., Farhadi, A., 2016. Unsupervised deep embedding for clustering analysis, in: International Conference on Machine Learning, PMLR. pp. 478–487.
- Yang, Y., Xu, Z., 2020. Rethinking the value of labels for improving class-imbalanced learning. *Advances in Neural Information Processing Systems* 33, 19290–19301.
- Yin, T., Wang, J., Zhao, Y., Wang, H., Ma, Y., Liu, M., 2025. Fine-grained adaptive contrastive learning for unsupervised feature extraction. *Neurocomputing* 618, 129014. URL: <https://www.sciencedirect.com/science/article/pii/S0925231224017855>, doi:<https://doi.org/10.1016/j.neucom.2024.129014>.
- Zhang, D., Nan, F., Wei, X., Li, S.W., Zhu, H., McKeown, K., Nallapati, R., Arnold, A.O., Xiang, B., 2021. Supporting clustering with contrastive learning, in: Proceedings of the 2021 Conference of the North American Chapter of the Association for Computational Linguistics: Human Language Technologies, Association for Computational Linguistics, Online. pp. 5419–5430. URL: <https://aclanthology.org/2021.naacl-main.427>, doi:10.18653/v1/2021.naacl-main.427.
- Zhang, Z., Tian, H., Jin, J., 2024. Multiple adaptive over-sampling for imbalanced data evidential classification. *Engineering Applications of Artificial Intelligence* 133, 108532. URL: <https://www.sciencedirect.com/science/article/pii/S0952197624006900>, doi:<https://doi.org/10.1016/j.engappai.2024.108532>.
- Zhou, B., Lapedriza, A., Khosla, A., Oliva, A., Torralba, A., 2017. Places: A 10 million image database for scene recognition. *IEEE Transactions on Pattern Analysis and Machine Intelligence* 40, 1452–1464.
- Zhou, Z., Yao, J., Wang, Y.F., Han, B., Zhang, Y., 2022. Contrastive learning with boosted memorization, in: Chaudhuri, K., Jegelka, S., Song, L., Szepesvari, C., Niu, G., Sabato, S. (Eds.), Proceedings of the 39th International Conference on Machine Learning, PMLR. pp. 27367–27377. URL: <https://proceedings.mlr.press/v162/zhou221.html>.